LIMNOLOGY and OCEANOGRAPHY

ASLO

Limnol. Oceanogr. 9999, 2020, 1–15

doi: 10.1002/lno.11409

Bacterioplankton metabolism of phytoplankton lysates across a cyclone-anticyclone eddy dipole impacts the cycling of semi-labile organic matter in the photic zone

Emma K. Wear [1]*, **Craig A. Carlson** [2], **Matthew J. Church** [1,3]

[1]Flathead Lake Biological Station, University of Montana, Polson, Montana
[2]Department of Ecology, Evolution, and Marine Biology and Marine Science Institute, University of California, Santa Barbara, California
[3]Division of Biological Sciences, University of Montana, Missoula, Montana

Abstract

Mesoscale eddies, prominent physical processes in the stratified ocean gyres, affect community composition and metabolic rates of both phytoplankton and heterotrophic bacterioplankton (free-living bacterial and archaeal) communities. We hypothesized that in situ differences in organic matter production would predispose bacterioplankton communities from cyclonic vs. anticyclonic eddies toward metabolic capabilities better suited to utilizing dissolved organic matter (DOM) from the phytoplankton groups commonly associated with each eddy polarity. To test this, we established dilution batch-culture bioassay incubations along a cyclone to anticyclone spatial transect in the North Pacific Subtropical Gyre. Unamended incubations, to assess spatial variability in ambient DOM bioavailability, and incubations amended with lysates of phytoplankton cultures were established and community growth and metabolic responses were assessed. Over timescales of days, lysate type was more influential than incubation origin: *Prochlorococcus* lysate was rapidly remineralized, while *Emiliania huxleyi* lysate was efficiently incorporated into biomass and developed a unique community of copiotrophic bacteria. Over timescales of 1 week to 1 month, eddy effects were indirectly apparent in their potential to promote metabolic processes related to DOM production and consumption. Surface lysate incubations showed priming of ambient DOM, that is, the remineralization of DOM, which was otherwise not bioavailable, in the presence of labile substrates. Some incubations originating from the deep chlorophyll maximum demonstrated signatures of chemoautotrophy fueled by nitrification, coincident with eddy-driven isopycnal uplift. We conclude that eddy polarity itself does not determine community-level bacterioplankton metabolic capabilities; however, mesoscale processes may indirectly affect slower, semi-labile organic matter processing in the oligotrophic ocean.

Mesoscale eddies, ocean vortices at size scales of around 100–200 km, are major drivers of biogeochemical processes in the surfaces of the oligotrophic gyres. Eddy-driven nutrient flux into the euphotic zone may account for as much as half of new primary production in the North Atlantic (McGillicuddy et al. 1998) and may be more influential in persistently stratified systems such as the North Pacific Subtropical Gyre (NPSG) that lack seasonality in deep mixing (Letelier et al. 2000). Ascani et al. (2013) argued that nitrate concentrations, and related oxygen concentrations, in the lower euphotic zone near Station ALOHA (the sampling site of the Hawaii Ocean Time-series [HOT] in the NPSG) are best explained by isopycnal depths as controlled by eddy variability. Near-monthly, substantial nitrate entrainment events have been observed by profiling floats in conjunction with eddy-driven isopycnal shoaling near Station ALOHA (Johnson et al. 2010).

Eddy effects on communities of primary producers are well characterized. Cyclones in the northern hemisphere canonically prompt centralized phytoplankton blooms by inducing isopycnal uplift of nutrient-rich waters into the sunlit layers of the upper ocean while anticyclones may promote phytoplankton blooms around their perimeters (McGillicuddy 2016). Cyclonic eddies are more often observed to enrich larger eukaryotic phytoplankton such as diatoms and haptophytes including coccolithophores (Letelier et al. 2000; Vaillancourt et al. 2003; Rii et al. 2008). Relative to conditions outside of the eddies, cyclones tend to select against the cyanobacteria *Prochlorococcus*

*Correspondence: emma.wear@flbs.umt.edu

Additional Supporting Information may be found in the online version of this article.

(Vaillancourt et al. 2003), while both relative enhancements (Sweeney et al. 2003) and decreases (Vaillancourt et al. 2003) in *Synechococcus* have been observed in cyclones. In contrast, anticyclonic eddies have been observed to favor *Prochlorococcus* (Cotti-Rausch et al. 2016) and nitrogen-fixing cyanobacteria (Fong et al. 2008; Church et al. 2009). However, the nuances of which specific phytoplankton are enriched, and to what degree, within a particular eddy at a given time are complex and likely influenced by factors such as eddy age, the relative strength of isopycnal displacement, and upwelling or downwelling rates (Sweeney et al. 2003; Benitez-Nelson and McGillicuddy 2008). In addition to intra-eddy horizontal variability in phytoplankton communities between the edges and center, effects on phytoplankton also vary vertically from the nutrient-depleted, well-lit surface waters to the base of the euphotic zone and deep chlorophyll maximum (DCM), where nutrient influx is more pronounced (Rii et al. 2008; Cotti-Rausch et al. 2016).

Given their physical and biogeochemical effects, it follows that mesoscale eddies have also been shown to affect heterotrophic bacterioplankton (here, the free-living bacteria and archaea). Most directly, the physical displacement of isopycnals has been shown to move bacterioplankton upward or downward in the water column (Nelson et al. 2014; Yan et al. 2018). Eddies may also indirectly affect the bacterioplankton by perturbing the phytoplankton community that supplies organic matter to the heterotrophic microbes. Bacterioplankton abundance (Lochte and Pfannkuche 1987; Ewart et al. 2008) and production (Ewart et al. 2008) may or may not be enhanced within eddies, but these properties have repeatedly been observed to be related to the spatial distribution of phytoplankton biomass within eddies. Likewise, bacterioplankton community composition (BCC) sampled during eddy-induced diatom blooms has been seen to shift toward phyla known to be copiotrophs (here, defined as r-strategists capable of responding rapidly to the input of a limiting organic nutrient) or phyla commonly associated with phytoplankton (Benitez-Nelson et al. 2007; Nelson et al. 2014). Thus, shifts in both phytoplankton abundance and community composition are likely mechanisms through which eddies could indirectly impact the metabolism and composition of the bacterioplankton. These effects may be particularly important in the stratified ocean gyres where the ambient dissolved organic matter (DOM) pool is of limited bioavailability and labile compounds are rapidly consumed (Carlson et al. 2002; Hansell 2013). For example, increased net community production has been inferred to accumulate as dissolved organic carbon in the euphotic zone of cyclonic eddies rather than solely fueling rapid particulate export (Benitez-Nelson et al. 2007; Chen et al. 2008).

We hypothesized that these known effects of mesoscale eddies, both on phytoplankton productivity and on bacterioplankton community metabolism and BCC, would translate to differential heterotrophic responses to DOM in cyclonic vs. anticyclonic eddies. That is, community-level preconditioning by in situ organic matter of variable composition or quality could lead to different realized heterotrophic metabolisms and presence of phylogenetic groups capable of variable responses to input of organic matter. To test this, we established a series of dilution batch-culture bioassays along a spatial transect across a cyclone-anticyclone eddy dipole in the NPSG. Unamended bioassay incubations, to assess spatial variability in ambient DOM bioavailability, and incubations amended with lysates of marine phytoplankton cultures were established and community growth and metabolic responses were assessed.

Methods

Experimental design

Incubations were established 02–06 April 2018, on a Simons Collaboration on Ocean Processes and Ecology (SCOPE) cruise on the R/V *Falkor* (FK180310). The cruise occupied the center of a cyclonic eddy then transited to the center of an anticyclonic eddy north of the Hawaiian Islands (Fig. 1A; Supporting Information Table S1). The five stations sampled targeted the center and edge of each eddy, as well as the neutral sea state between the eddies, which were identified and tracked by minima and maxima of sea surface height anomaly from the Copernicus Marine Environmental Monitoring Service (CMEMS: http://marine.copernicus.eu; anomalies reported herein are from the Global Ocean Gridded

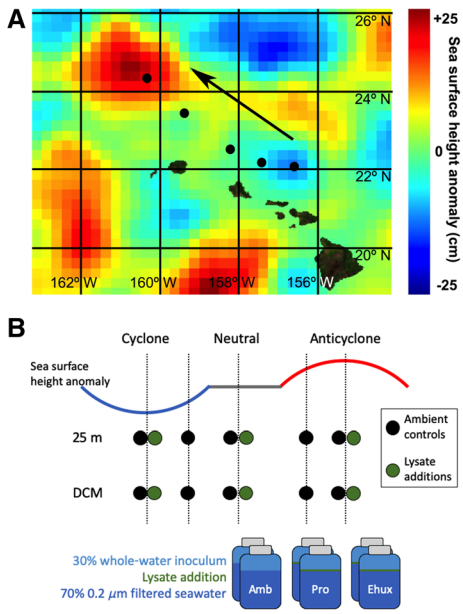

Fig. 1. (**A**) Contour plot of satellite-derived sea surface height anomalies on 04 April 2018, the temporal midpoint of the transect. Black dots indicate sampling locations and arrow denotes direction of travel. Note that sea surface height anomalies at sampling locations differ slightly from those in Supporting Information Table S1, due to the time-dynamic nature of the sampled eddies. Map modified from CMEMS (see Methods). (**B**) Schematic of incubation initiations across the eddy dipole (not to scale).

L4 Sea Surface Heights and Derived Variables NRT composite product SEALEVEL_GLO_PHY_L4_NRT_OBSERVATIONS_008_046). At the time of sampling, the cyclonic eddy was approximately 7 months old and weakening, while the anticyclone had persisted for approximately 3 months and was maintaining a stable intensity (B. Barone pers. comm.). Sampling was conducted with a rosette equipped with twenty-four 12 L Niskin bottles and an SBE 9 Plus conductivity-temperature-depth (CTD) sensor. A Wet Labs ECO-FLNTU fluorometer on the CTD was calibrated with discrete samples for chlorophyll pigments (termed chloropigments), inclusive of chlorophylls *a* and *b* (Karl et al. 2001). Upper-ocean profiles from 5 to 175 m were collected at each station from the same rosette cast as the experimental media to document in situ conditions in organic matter concentrations, bacterial abundance, and BCC.

Sterile seawater media was prepared by gravity-filtering directly from Niskin bottles using a 0.2 μm pore size, 142 mm mixed cellulose ester filter (Millipore GSMP, flushed with at least 1 L of ultrapure water followed by seawater) in a polycarbonate filter holder, into a media-rinsed high-density polyethylene carboy. Incubation bottles (1 L polycarbonate bottles washed with 10% hydrochloric acid) were rinsed three times with media and then filled with 700 mL of media and 300 mL of whole water (i.e., the bacterioplankton inoculum) from the same depth. Duplicate incubations were prepared from both 25 m and the DCM at each station to measure the bioavailability of ambient DOM (hereafter, ambient controls).

At the two eddy centers and the neutral sea-state station, four additional incubation bottles per depth were prepared as above and duplicates were spiked with one of two lysates prepared from phytoplankton cultures (Fig. 1B). We selected two representative phytoplankton based on time-series observations from Station ALOHA, where *Prochlorococcus* abundance near the DCM is positively correlated with sea surface height anomaly and eukaryotic phytoplankton abundance is negatively correlated with sea surface height anomaly (Barone et al. 2019). A *Prochlorococcus* lysate (hereafter, Pro) was prepared from axenic MIT1314, a High Light II culture originally collected from Station ALOHA north of Hawaii, that was grown in Pro99 medium (Moore et al. 2007). An *Emiliania huxleyi* lysate (hereafter, Ehux) was prepared using a nonaxenic environmental isolate (T. Ladd pers. comm.) from the Santa Barbara Channel, CA, grown in artificial seawater with modified "f" medium nutrients (Ladd et al. 2018). *E. huxleyi* is ubiquitous in this region, with higher abundances in the mid-photic zone and in the early spring, where it appears to exploit a low-nitrate niche (Cortés et al. 2001). Both cell types were pelleted by centrifugation, washed in unamended seawater or nutrient-free artificial seawater to remove nutrient carryover from the growth medium, lysed by freeze-thawing in ultrapure water, and filtered to remove particulates (see Supplemental Methods). Lysates were stored frozen until immediately before use. The Pro lysate targeted an ~3.5 μM TOC enrichment (2.5 μL of a 1.48 mM TOC stock per 1 L experiment; see SI Table 6) and the Ehux lysate targeted an ~ 10 μM TOC enrichment (4 μL of a 2.5 mM TOC stock), with each lysate enrichment determined by the respective phytoplankton culture yield.

Experiments were conducted in the dark using upright, shipboard incubators. While conducting these experiments in the dark was necessary to prevent carbon fixation by photoautotrophy, lack of light would have also inhibited photoheterotrophy, thereby potentially underestimating total heterotrophic activity. Incubators were kept at ambient temperatures for the cyclone (23°C for 25 m and 21.5°C for the DCM; across the transect, these were within 0.4°C of in situ temperatures at 25 m and within 1.1°C at the DCM, Supporting Information Table S2). At the end of the cruise, incubators were transferred to an onshore laboratory for further sampling. Incubations were subsampled by gently swirling then decanting daily for 1 week and then again at 34 d, a nominal one-month timepoint (Supporting Information Table S3).

Organic matter quantification

Samples for measurement of organic matter concentrations were collected in combusted (500°C for 4 or more hours) borosilicate vials with Teflon-lined silicone septa, acidified with 4 N hydrochloric acid to a pH of 2–3, and stored at room temperature in the dark. To minimize the risk of contamination during handling, samples were not filtered and thus represent the total organic pool, including bacterioplankton biomass. Total organic carbon (TOC) and total nitrogen (TN) were measured by high temperature combustion using modified Shimadzu TOC-Vs and TOC-Ls with a Shimadzu Total N module. Based on a realized analytical precision of 1–2% and the performance of reference materials throughout the runs, we can resolve differences in TOC of 1.5 μM and in TN of 1 μM. All samples were referenced against surface and deep seawater every six to eight samples during analysis, and reference seawater was calibrated with consensus reference material provided by D. Hansell (University of Miami; Hansell 2005).

Samples for subsequent analysis of dissolved inorganic nitrogen (DIN) from the incubations were collected in acid-washed high-density polyethylene bottles and stored frozen at −20°C before flow injection analysis using a QuikChem 8500 Series 2 (Lachat Instruments; detection limits: $NO_2^- + NO_3^-$, 0.2 μM; NO_2^-, NH_4^+, and PO_4^{3-}, 0.1 μM) at the University of California, Santa Barbara Marine Science Institute Analytical Lab. Measurements that were below detection limit were set to the detection limit to be conservative. Total organic nitrogen (TON) was estimated by subtracting DIN from TN. DIN concentrations were only available for a subset of field samples; where measured, $NO_2^- + NO_3^-$ was at nanomolar concentrations at 25 m to a maximum of 0.1 μM at the DCM (D. Karl pers. comm; http://scope.soest.hawaii.edu). We therefore estimated in situ TON concentrations using the initial DIN concentrations in our ambient controls; this is a likely underestimate of TON, but we note that anticipated DIN

concentrations were less than the error of our TN measurements. Total hydrolyzable amino acids (THAA) in lysates were quantified via high performance liquid chromatography (see Supplemental Methods).

Bacterial abundance

Samples for bacterial abundance were preserved with a final concentration of 0.8% paraformaldehyde (Electron Microscopy Sciences) and stored frozen at −80°C. Bacterial abundance was determined using an Attune acoustic focusing cytometer (Applied Biosystems model), with SYBR Green II staining for total cell counts (Supporting Information Fig. S1). As experiments were conducted in the dark, changes in cell abundance were attributed to heterotrophic and chemoautotrophic organisms, and thus photoautotrophic cells were not independently enumerated.

Bacterial community composition and *amoA* gene abundance

DNA samples for subsequent assessment of bacterioplankton community composition (BCC) from field samples (1 L) were collected under gentle peristaltic pressure onto 0.2 μm pore size, 25 mm polyethersulfone filters (Supor, Pall), which were stored dry at −80°C. Due to volume constraints, DNA sampled from incubations at day 3 was combined between duplicates (300 mL per replicate) and filtered as were the field samples. Samples were lysed by freeze-thawing and bead-beating in a Biospec Mini-Beadbeater-16, and genomic DNA was extracted using the MasterPure Complete DNA and RNA Purification Kit (Lucigen). 16S rRNA genes were amplified using multiplexed primers targeting the V4-5 hypervariable region: 515F-Y (5′-GTGYCA GCMGCCGCGGTAA-3′) and 926R (5′-CCGYCAATTYMTTT RAGTTT-3′), as recommended by Parada et al. (2016), with an index on the forward primer following the design of the Earth Microbiome Project (Caporaso et al. 2012). Amplicons were sequenced on an Illumina MiSeq using PE250 v2 chemistry. Operational taxonomic units (OTUs, 99% similarity level) were generated using mothur v1.39.5 (Schloss et al. 2009) and classified using SILVA v132 (Quast et al. 2013). Weighted UniFrac distance (Lozupone and Knight 2005), which accounts for phylogenetic relatedness of OTUs as well as for relative abundance, was used to calculate distances between samples. For full sequencing methods, including amplification conditions and bioinformatics details, see Supplemental Methods.

Droplet digital PCR (ddPCR; Bio-Rad QX200 system) was used to quantify archaeal ammonia monooxygenase subunit A (*amoA*) genes from field samples (see Supplemental Methods). We used the two sets of primers designed by Beman et al. (2008), which target *amoA* genes specific to shallow (Group A) and deep (Group B) clades of ammonia-oxidizing archaea.

Calculations and statistics

Bacterioplankton specific growth rates (μ) were calculated as the rate of change of the natural log of cell abundance during either the exponential growth phase or the first week of the experiment if cell abundance did not reach stationary phase of growth during that time (as was the case in some ambient controls).

Bacterial growth efficiency (BGE) was calculated as:

$$\mathrm{BGE} = \left[(\mathrm{BB_{stationary}} - \mathrm{BB_{lag}})*(\text{days to stationary phase})^{-1}\right] * \left[((\mathrm{TOC_{T0}} - \mathrm{BB_{T0}}) - (\mathrm{TOC_{T3}} - \mathrm{BB_{T3}}))*(\text{days to T3})^{-1}\right]^{-1} * 100$$

where T0 and T3 are the initial and three-day sampling timepoints, respectively. Bacterioplankton biomass at T0 (BB_{T0}) and during the lag phase (BB_{lag}) was estimated from cell abundance using conversion factors of 10 fg C cell^{-1} (Christian and Karl 1994; Fukuda et al. 1998) and at stationary phase ($BB_{stationary}$) and T3 (BB_{T3}) using 17 fg C cell^{-1} (adjusted from T0 using cell biovolumes determined by microscopy; see Supplemental Methods). Because the Pro lysate contained cellular debris that interfered with cell enumeration at T0, the mean T0 cell abundance from the corresponding Ehux incubations was used for Pro incubations.

Statistics were conducted in SPSS Statistics v25 (IBM) and Primer v6 (Clarke and Gorley 2006). Contour plots were produced with Ocean Data View v5.1.5 (Schlitzer 2018).

Results

In situ conditions

When samples for incubations were collected, the satellite-based sea surface height anomaly near the center of the cyclone was −10 cm, while the anticyclone had stronger isopycnal displacement with a sea surface height anomaly of +23 cm (Supporting Information Table S1). Physicochemical conditions at 25 m were generally constant across the transect, while at the DCM, the decrease in isopycnal uplift from the center of the cyclone toward the center of the anticyclone was reflected in physicochemical gradients across the transect (Fig. 2; Supporting Information Table S2). As expected for an oligotrophic gyre, chloropigment concentrations were lower at 25 m than at the DCM, while TOC concentrations were 3–10 μM higher at 25 m. Bacterioplankton abundances were higher and moderately more variable at 25 m (5.2×10^5 to 6.3×10^5 cells mL^{-1}) than at the DCM (3.7×10^5 to 4.5×10^5 cells mL^{-1}).

Eddy-related spatial changes in the vertical position of isopycnal surfaces strongly influenced physicochemical conditions in the waters from which the DCM incubations were established (Fig. 2; Supporting Information Table S2). The depth of the DCM varied between 100 and 130 m and crossed isopycnals along the transect; within this feature, chloropigment concentrations were elevated in the cyclone (1.0 and 1.2 μg L^{-1}

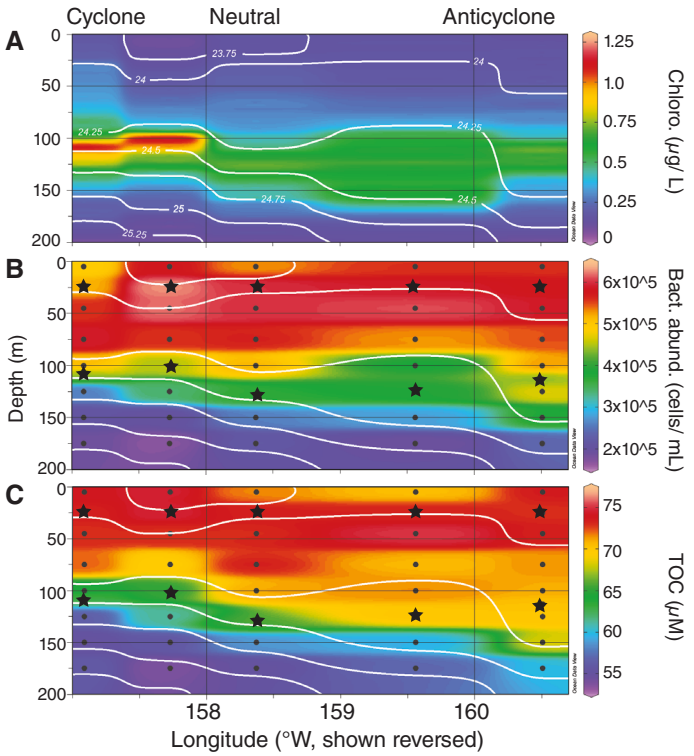

Fig. 2. Contour plots of in situ conditions during the eddy dipole sampling transect as shown in Fig. 1A. Note that longitude on the X-axis is reversed to match subsequent figs. (**A**) Concentration of chloropigment. (**B**) Bacterioplankton abundance. (**C**) TOC concentration. White contours are isopycnal surfaces (kg m^{-3}), with all density contours as labeled in panel A; black dots indicate where field samples were collected and black stars denote the depths from which incubations were established.

in the center and edge, vs. 0.7 μg L^{-1} at the neutral and anticyclone sites; Fig. 2). TOC concentrations were higher in the DCM of the anticyclone (70 μM at both the eddy edge and center, vs. 63–66 μM in the cyclone and neutral stations). TON was relatively constant across the transect (4.2–4.9 μM at the DCM), with the end result that TOC:TON was likewise elevated in the DCM of the anticyclone eddy center (16.6, vs. 12.9 at the cyclone center and 14.8–15.1 at the neutral and eddy edge stations).

Experiment starting conditions

We established 22 duplicated incubations across the transect: 10 pairs measuring bioavailability of naturally occurring DOM in unamended seawater, called ambient controls, and six pairs each measuring responses to added Pro or Ehux lysates. Starting concentrations of TOC and TN varied with location and depth, following the in situ patterns, as well as with lysate treatment (Fig. 3A; Supporting Information Fig. S2). The median differences between in situ concentrations and the starting (T0) concentrations in the corresponding ambient controls after experimental setup were 1 μM for TOC (range of −1.3 to 2.3 μM) and −0.2 μM for TN (range −0.6 to 0.3), indicating that handling effects were minimal. Ambient control incubations started with PO_4^{3-} concentrations consistently below detection limits and DIN concentrations ranging from below detection limits to 0.5 μM. $NO_2^- + NO_3^-$ was only detected in the DCM of the cyclone and neutral sea-state incubations, while the distribution of NH_4^+ was not depth- or eddy-dependent (Supporting Information Table S5).

The addition of *Prochlorococcus* lysate (Pro treatment) resulted in a median enrichment of 3.4 μM TOC and 0.5 μM TN relative to the corresponding ambient DOM incubations, while incubations amended with lysate from *E. huxleyi* (Ehux treatment) had a median enrichment of 8.2 μM TOC and 3.6 μM TN (Supporting Information Table S5 and Table S6). The nitrogen added with the Ehux lysate was primarily organic, with a median addition of 0.3 μM NH_4^+ and no detectable $NO_2^- + NO_3^-$ addition, while the Pro lysate had no detectable DIN. The Ehux lysate had a notably low TOC:TON ratio for phytoplankton lysate (a median of 2.5 as measured in the incubations, vs. 6.4 for the Pro lysate). Both lysates contained a high percentage of TN as amino acids (~60% in Ehux and ~75% in Pro, based on molarity of N), although the overall concentration added with the Ehux lysate was much higher (2.6 μM N as amino acids, vs. 0.3 μM with the Pro lysate; Supporting Information Table S6) and the relative contribution of specific amino acids varied between lysates (Supporting Information Table S7).

TOC remineralization

Ambient control incubations in general did not show resolvable TOC remineralization over the duration of the experiment (Fig. 3C,E,G; Supporting Information Table S5). Only three individual replicates had resolvable TOC drawdown of 1.5 μM or greater after 1 month, and in no case was this duplicated.

In contrast, all of the lysate addition incubations showed resolvable TOC remineralization of 1.7 to 5.4 μM by the 3-day timepoint (Fig. 3C). Because in situ TOC concentrations varied spatially and TOC amendments varied between lysate types, remineralization in the lysate treatments was normalized to the amount of TOC added in each particular incubation (the difference between starting [TOC] in an incubation minus the median starting [TOC] in the corresponding ambient DOM incubations) to calculate percent lysate remineralized ($\%_{lys}$). At day 3, 43% to 133%$_{lys}$ was remineralized (Fig. 3D), with the greatest $\%_{lys}$ remineralization in the cyclone Pro experiments at both depths. By the end of 1 week, 50% to 107%$_{lys}$ was remineralized (Fig. 3F). Effects of lysate type were no longer apparent after 1 week, but there was an overall trend toward higher percent remineralization, when compared within lysate-depth combinations, in the anticyclone incubations and lower remineralization in the neutral sea-state incubations, particularly in those established from 25 m (Fig. 3F).

After 1 month of incubation, 17% to 232%$_{lys}$, or TOC concentrations between no measurable change and 11.0 μM, had been remineralized (Fig. 3G,H). Anticyclone incubations within

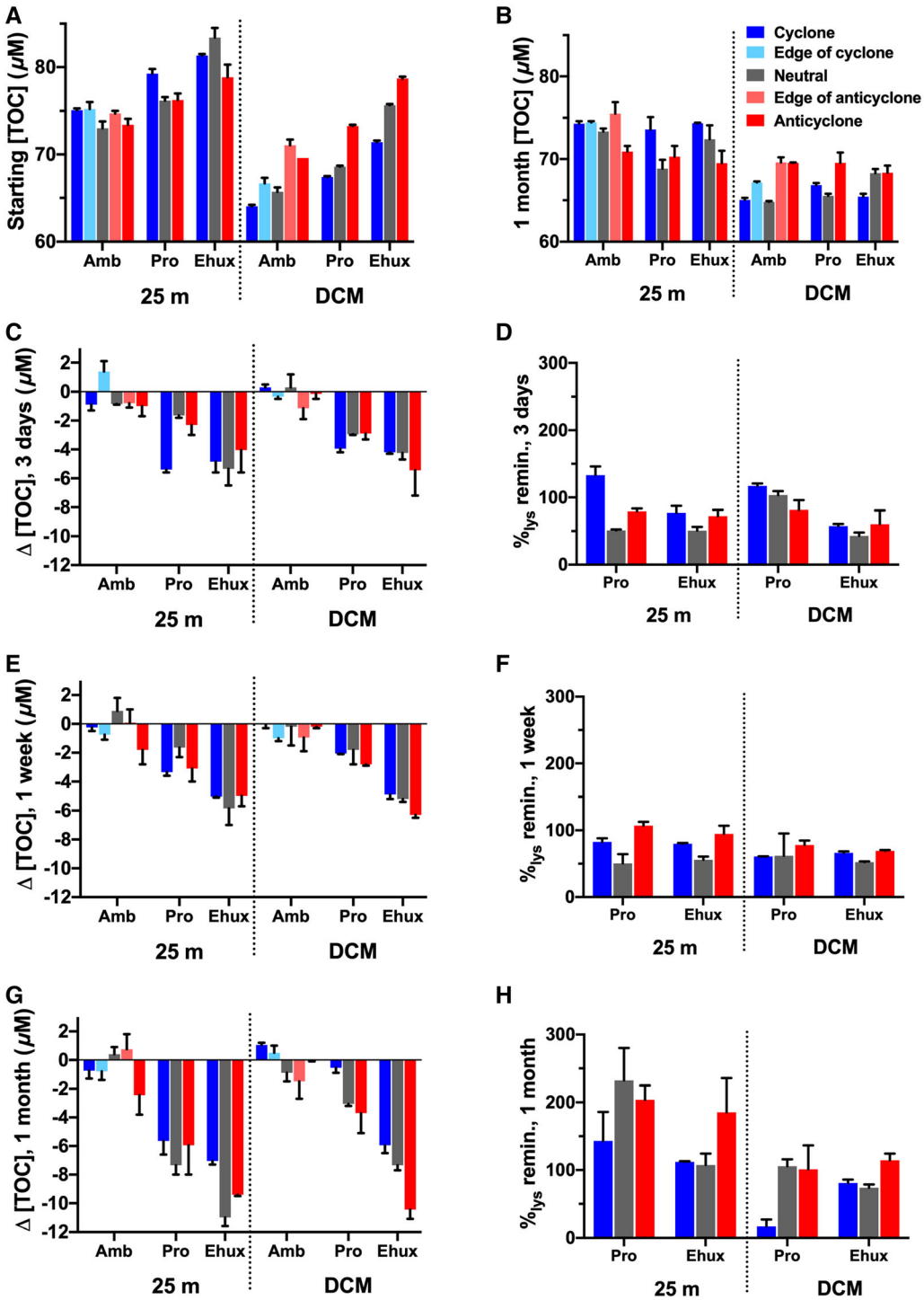

Fig. 3. TOC concentrations and remineralization in incubations. (**A**) Starting TOC concentrations in incubations. (**B**) TOC concentrations at final, 1-month timepoint. (**C**, **E**, and **G**) Change in TOC concentration from starting concentration to 3-day, 1-week, and 1-month timepoints. (**D**, **F**, and **H**) TOC remineralization in lysate addition incubations, expressed as $\%_{lys}$, or the percent of TOC added as lysate remineralized by the 3-day, 1-week, and 1-month timepoints. Columns indicate median of duplicate incubations and error bars indicate range.

lysate-depth groupings had consistently higher $\%_{lys}$ remineralization than corresponding cyclone incubations, while neutral sea-state incubations were variable. TOC concentrations in the lysate incubations were on the whole similar to those in the corresponding ambient controls, indicating a total remineralization of added TOC after 1 month; however, individual

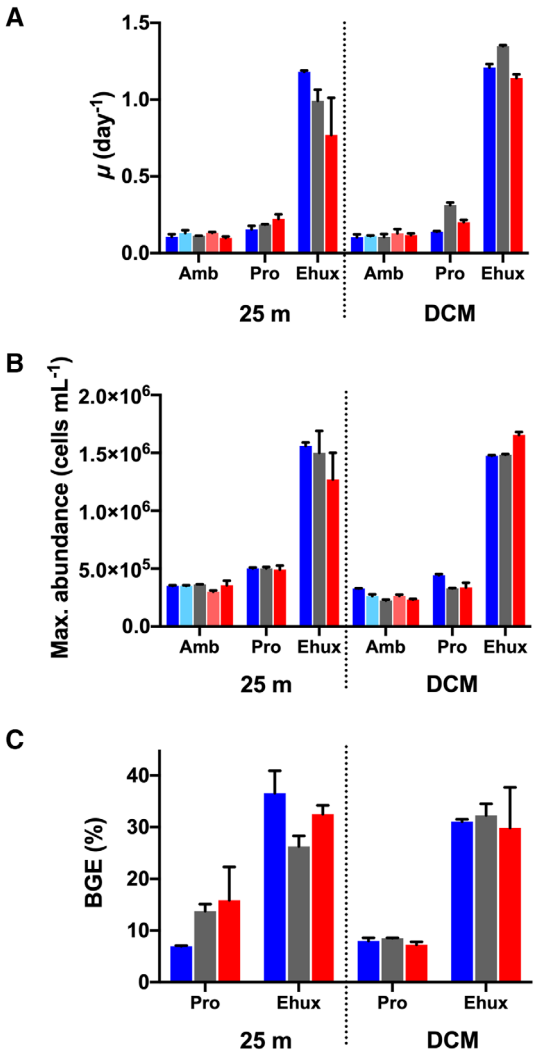

Fig. 4. Cellular growth properties. (**A**) μ, specific growth rate. (**B**) Maximum bacterial abundance. (**C**) Bacterial growth efficiencies. BGEs could not be calculated for ambient controls due to low rates of remineralization. Legend as in Fig. 3. Columns indicate median of duplicate incubations and error bars indicate range.

replicates had as much as 4 μM more or 5.5 μM less TOC than the ambient DOM incubations (Fig. 3B). In some Pro incubations from the DCM, TOC increased from the 3-day or 1-week timepoint to the 1-month timepoint, decreasing the apparent remineralization; we discuss possible interpretations below.

Short-term growth responses and BCC shifts

For short-term growth responses, treatment type outweighed any site-specific factors. Specific growth rates (μ; Fig. 4A) were significantly different between all treatments (Kruskal-Wallis H = 18.369, df = 2, p = 0.0001; followed by pairwise Mann–Whitney U-tests, all $p \leq 0.004$), with no consistent pattern between depths. Growth rates in ambient controls were between 0.10 and 0.13 d^{-1} (mean 0.11 d^{-1}); on Pro lysate, 0.14 to 0.31 d^{-1} (mean 0.20 d^{-1}); and on Ehux lysate, 0.77 to 1.35 d^{-1} (mean 1.11 d^{-1}). Maximum bacterioplankton abundances observed at stationary phase or over 1 week (Fig. 4B) likewise were significantly different between treatments (Kruskal-Wallis test H = 15.600, df = 2, p = 0.0004; followed by pairwise Mann–Whitney U-tests, all $p \leq 0.017$), with maximum abundances in the Ehux incubations three to five times greater than those in the other treatments. Maximum abundance was generally but not significantly higher in 25 m incubations than in DCM incubations from the same station and treatment (Wilcoxon Signed Rank Test Z = −1.956, p = 0.050).

BGEs were also closely related to lysate addition type, with no consistent effect of source location. BGEs were significantly higher (Mann–Whitney U = 0, p = 0.004) in the Ehux treatments (mean 31%) than in the Pro treatments (mean 10%). BGEs could not be calculated for ambient controls as remineralized TOC was below detection limits.

Bacterial community composition at day 3 of the experiments reflected the tendency for treatment effects to overwhelm potential experiment source water effects (Fig. 5; Supporting Information Fig. S3A). We focus here on BCC with cyanobacterial sequences removed bioinformatically, as changes in photoautotroph abundance in the experiments would likely reflect lack of light rather than lysate treatment (although we note that BCC shifts in experiments were qualitatively similar with cyanobacteria included; Supporting Information Fig. S3B). At the 3-day timepoint in our experiments, the 25 m ambient controls were most similar to in situ communities, followed by the DCM ambient controls (Fig. 5; Supporting Information Fig. S3A). Proincubation communities changed a moderate amount and retained some depth differentiation, while Ehux lysate produced communities that were the most different from in situ communities but most similar to one another within the treatment, regardless of starting location or depth (Fig. 5; Supporting Information Fig. S3A).

BCC shifts were driven by increases in putative copiotrophic OTUs, and concomitant relative declines in SAR11 OTUs, in the experimental incubations (Fig. 5; Supporting Information Table S8). The 25 m ambient controls remained SAR11-dominated, similar to their in situ counterparts, but showed a slight increase in presumed copiotrophic *Gammaproteobacteria*. The DCM ambient controls showed a decrease in a *Euryarchaeota* OTU and a more pronounced increase in *Gammaproteobacteria*. Both lysate addition types stimulated increases in *Rhodobacteraceae*; a *Shimia* sp. OTU was present in all experiments, and other genera were sporadically detected. The Pro lysate stimulated higher relative abundance of an *Alteromonas* sp. OTU, while the Ehux incubations were heavily dominated by a *Vibrio* sp. OTU.

Nitrogen dynamics

TN concentrations remained within 1.1 μM of starting concentrations over the course of the incubations (median change of −0.2 μM; Supporting Information Fig. S2C). DIN and,

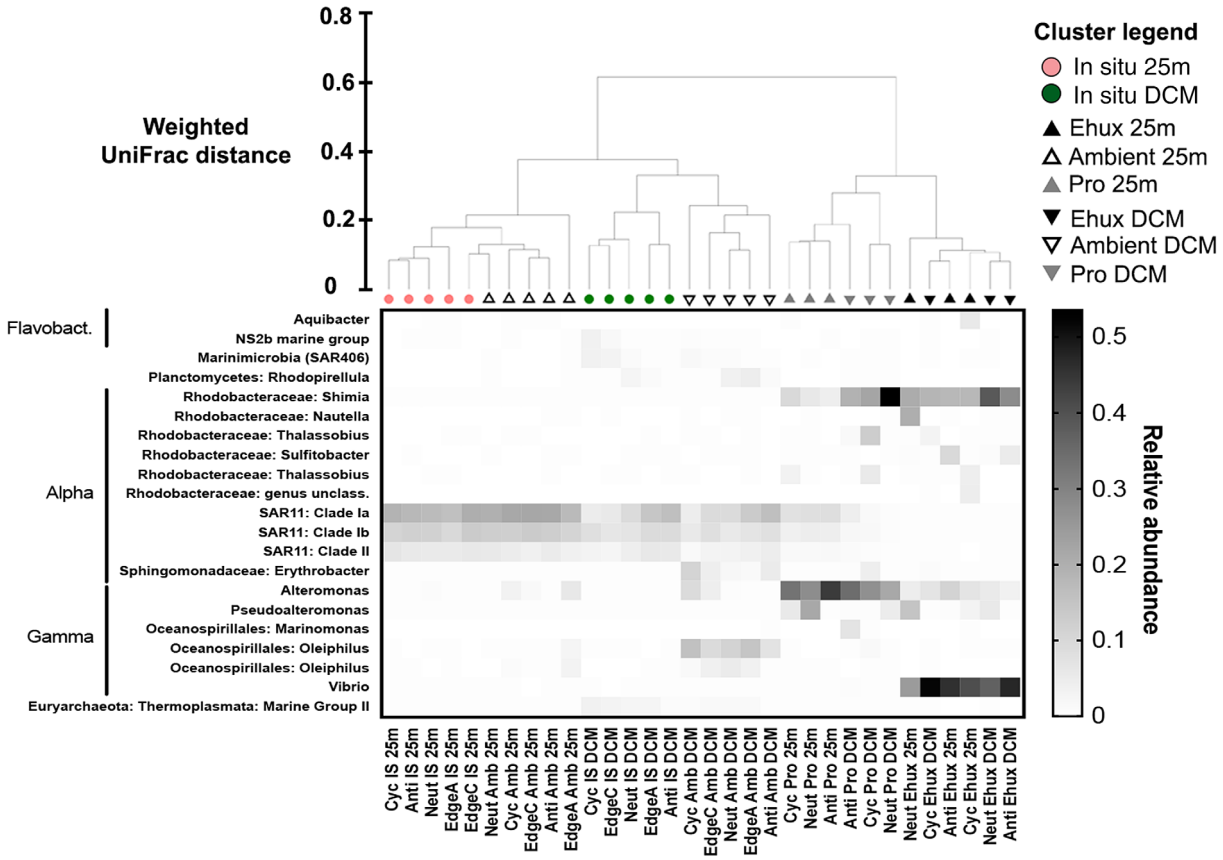

Fig. 5. Relative abundance of major OTUs in the incubations at day 3 and in the corresponding field samples from which incubations were established. OTUs shown are all those present at a relative abundance of 0.03 or greater in at least one experimental or corresponding in situ sample. Flavobact. = *Flavobacteriaceae*; Alpha = *Alphaproteobacteria*; Gamma = *Gammaproteobacteria*. For full phylogenetic identification, see Supporting Information Table S8. [Color figure can be viewed at wileyonlinelibrary.com]

correspondingly, TON concentrations were more variable between treatments. At 1 month, the ambient controls demonstrated no net change in NH_4^+ and $NO_2^- + NO_3^-$ concentrations and a slight median decrease in TON (–0.2 μM, within detection limits of TN). The Pro lysate incubations accumulated a median of 0.1 μM NH_4^+ (range of –0.1 to 0.32 μM) and overall had no net change in $NO_2^- + NO_3^-$ concentrations (range of 0 to 0.2 μM) after 1 month, with median changes of 0.2 μM DIN and –0.1 μM TON. The Ehux incubations consistently converted substantial TON (median change of –2.6 μM, range –4.6 to –1.0 μM) into DIN (median gain of 2.4 μM, range 1.3 to 3.6 μM), mostly in the form of NH_4^+ (median 2.0 μM, range –0.5 to 2.7 μM) but with notable increases in $NO_2^- + NO_3^-$ concentrations in a few experiments (median 0.1 μM, range 0 to 4.2 μM).

The abundance of archaeal *amoA* genes was estimated from in situ DNA samples as an indicator of nitrification potential in starting communities (Fig. 6; Supporting Information Tables S2 and S4). Genes from both the shallow (Group A) and deep (Group B; Beman et al. 2008) clades were minimally present at

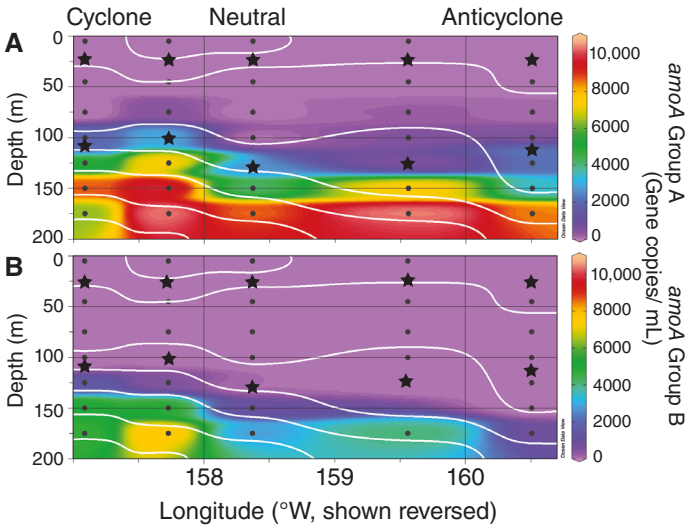

Fig. 6. Contour plots of in situ *amoA* gene abundances. (**A**) Shallow clade (Group A). (**B**) Deep clade (Group B); clade designations as in Beman et al. (2008). White lines are isopycnal surfaces (kg m^{-3}) as in Fig. 2A and black stars indicate locations from which experiments were established.

25 m (<15 copies mL^{-1}). At the DCM, the shallow clade *amoA* genes were two to three orders of magnitude higher than at 25 m (546 to 3009 copies mL^{-1}) while the deep clade *amoA* genes were at most present at 90 copies mL^{-1}. Both gene types increased in abundance below the DCM (Fig. 6).

Discussion

We observed large differences in how bacterioplankton responded to allochthonous phytoplankton lysates in a series of dilution batch-culture bioassays transecting an eddy-eddy dipole. The resulting short-term responses were more clearly related to the type of lysate addition and to the depth from which incubations were established than to the locations across the eddy dipole from which experimental seawater was collected. The low bioavailability of ambient TOC was consistent with our expectations for a stratified oligotrophic gyre, while the varying responses to lysates generated from *Prochlorococcus* and *E. huxleyi* cultures suggest different metabolic strategies in response to these substrate types. Our results further suggest that, after 1 month, both chemoautotrophy, likely fueled by nitrification, and priming of semi-labile DOM utilization had occurred in subsets of the lysate amendment incubations. While these processes complicate our interpretation of heterotrophic responses, extrapolating these amendment results to field conditions and potential responses to bursts of organic matter production associated with mesoscale features suggests unexpected ways that mesoscale processes could impact the oligotrophic ocean.

Short-term bacterial growth and remineralization responses

Short-term remineralization responses were strongly related to substrate type, with no clear effects of starting location other than between depth horizons. At the 3-day timepoint, the experiments showed comparable absolute TOC remineralization of both lysate types within starting depths, but the $\%_{lys}$ remineralized was much higher for the Pro incubations because of the smaller initial TOC addition. The responses between lysate types were qualitatively different in how the organic matter was directed into cellular growth and remineralization—the Pro lysate was rapidly remineralized, while bacterioplankton in the Ehux incubations showed significantly higher growth rates and BGEs, suggesting a physiologically distinct response to the two lysates. Differing bacterioplankton metabolic responses to lysates or exudates from different clades of phytoplankton, presumably due to differing quality as a substrate for growth, have been observed in a number of studies (e.g., Sarmento and Gasol 2012; Wear et al. 2015; James et al. 2017).

The differences in BGEs likely reflect differences in quality as well as quantity of the lysate additions. The lower C:N ratio of the Ehux lysate suggests higher quality as a growth substrate (del Giorgio and Cole 1998); in particular, the high concentrations of amino acids in the Ehux lysate (Supporting Information Table S6) could be readily partitioned to anabolism and facilitate increased cell division and biomass production (reviewed in Kirchman 1990; del Giorgio and Cole 1998). The distinct molar percentages of the amino acids between the lysates further indicates that there were compositional differences at the molecular level (Supporting Information Table S7), as would be expected for two such phylogenetically distinct phytoplankton sources (e.g., Becker et al. 2014). We speculate that the Pro lysate was more representative of a substrate typically encountered by resident bacterioplankton within a highly stratified oligotrophic water column and therefore did not drive a strong physiological shift from maintenance to biomass production. In contrast, the Ehux lysate appears to have prompted a more stereotypical bloom response, both metabolically and in BCC. It is also possible that the *Vibrio*-dominated community that developed in the Ehux lysate incubations (Fig. 5) was particularly influential in increasing BGEs; *Vibrio* in culture have been seen to maintain BGEs of 30–50% during aerobic growth, likely furthered by the clade's ability to engage in intracellular carbon storage (reviewed in Thompson and Polz 2006). Our choice of phytoplankton lysate rather than exudate was driven by methodological concerns. For example, to remove inorganic nutrients remaining in the phytoplankton growth media and to achieve the necessary amendment volume and concentration for our bioassay experiments, we would need to concentrate large volumes of exudates with solid phase extraction resin (Dittmar et al. 2008), a technique that could alter the molecular composition and thus bioavailability of the DOM. However, lysate is more representative of DOM that may be produced via bloom-associated and food web-mediated processes such as viral lysis and sloppy feeding (Carlson and Hansell 2015) and thus may also influence the nature of the responding community.

Short-term response in BCC

After 3 days of incubation, BCC responses reflected the differing bioavailability of the DOM treatments, with no obvious effect of the eddy state from which the starting communities were sampled. The Ehux incubations yielded higher specific growth rates and BGEs and correspondingly the highest production of new cells, and the resulting communities were the most different from in situ conditions. The Pro incubations showed an increase in the *Rhodobacteraceae* (commonly seen in association with phytoplankton: e.g., Amin et al. 2012) and a putative copiotrophic *Alteromonas* sp. OTU (frequent early responders in batch-culture-style experiments: McCarren et al. 2010; Nelson and Carlson 2012; Pedler et al. 2014), which were also present in the Ehux communities. The Ehux incubations also showed pronounced increases in the relative abundances of a *Vibrio* sp. OTU. *Vibrio* have been observed blooming in diverse coastal systems in response to phytoplankton blooms (Asplund et al. 2011; Gilbert et al. 2012; Main et al. 2015), particularly in association with diatoms, and in organic matter amendment experiments established

from subtropical gyres (Nelson and Carlson 2012; Zhang et al. 2019). We cannot distinguish the importance of lysate quality and composition vs. quantity in shaping BCC in these experiments, but the Ehux lysate in particular resulted in a clear and distinct bottom-up selective effect.

The ambient controls, despite a low specific growth rate and generally unmeasurable TOC remineralization, also showed a slight increase in putative copiotrophic OTUs, in particular the same *Alteromonas* OTU seen in the lysate addition communities and, in the DCM incubations, a member of the *Oceanospirillales*. These increases could derive from the initial release from grazing pressure in the incubations (e.g., Nelson and Wear 2014; Pedler et al. 2014).

Short-term remineralization: Spatial effects

At 1 week, the $\%_{lys}$ remineralized was generally higher in the cyclone and anticyclone incubations than in the corresponding neutral sea-state incubations. This is consistent with evidence that eddies in general, regardless of polarity, can in some cases enhance bacterioplankton activity relative to outside, neutral sites (Baltar et al. 2010). At the 1-week and 1-month timepoints, the anticyclone incubations trended toward higher total and $\%_{lys}$ remineralization than the corresponding cyclone incubations, regardless of lysate type. In the DCM incubations, this pattern likely reflects greater evidence for chemoautotrophy in the cyclone incubations, as discussed below; our observations do not suggest a clear explanation for why this pattern was also seen in the 25 m incubations.

Spatial patterns in bacterioplankton growth and remineralization across the eddy dipole were muted compared with the effects of lysate type and depth, suggesting that during our study eddy polarity was not a major factor shaping bacterioplankton community metabolic potential. We note that we did not sample a dipole with a pronounced gradient in chloropigment concentration (Fig. 2A) and that, at the time of sampling, satellite altimetry indicated that the anticyclone was stronger than the cyclone, which was coherent but beginning to weaken (B. Barone pers. comm.). We therefore cannot rule out the possibility that we would have seen an effect were we to conduct such an experiment across a dipole of two similarly aged, strong eddies; however, our experiment provides no evidence that bacterioplankton communities maintain substantial differences in metabolic potential over the life of an eddy.

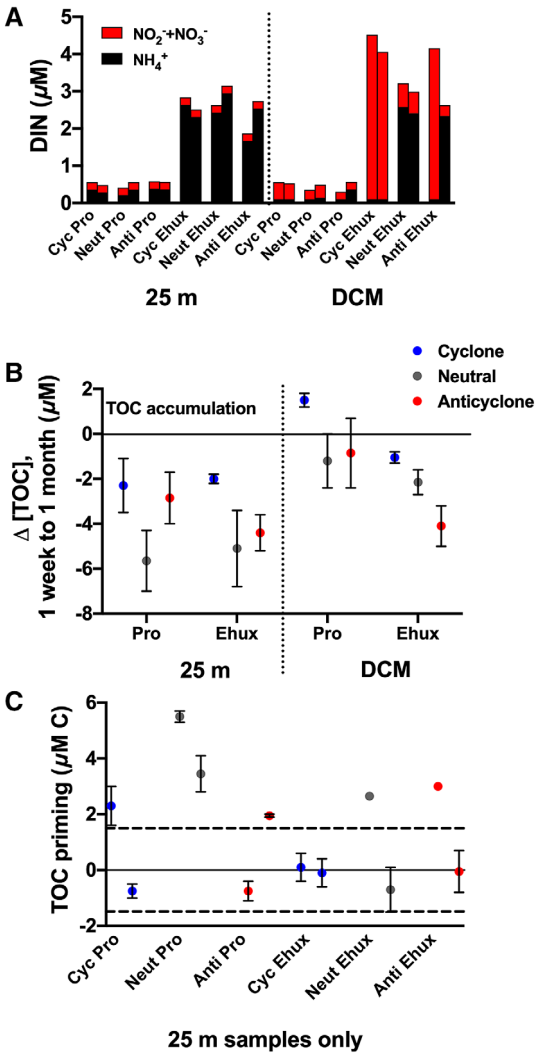

Fig. 7. Evidence of nitrification and priming at 1 month. (**A**) DIN speciation after 1 month in the lysate addition incubations (ambient control incubations are omitted for clarity). Note that individual replicates are reported here, as some treatments replicated poorly, and the legend differs from panels **B** and **C**. (**B**) Change in TOC concentration from 1 week to 1 month, in lysate addition incubations only. Dots indicate the median of duplicate incubations and error bars indicate the range. (**C**) TOC priming (such that primed remineralization is positive), in 25 m samples only. Both replicate incubations are shown; error bars are the range of duplicate analytical draws from each incubation. Dashed lines indicate the resolvable difference of 1.5 μM. Legend as in B.

Long-term remineralization: Potential chemoautotrophy

A small number of DCM lysate incubations showed an increase in TOC concentrations from the 3-day and 1-week to 1-month timepoints (Fig. 7B; Supporting Information Figs. S4 and S5). We emphasize that these were not net increases relative to starting TOC concentrations but rather increases relative to intermediate timepoints (Fig. 3G, Supporting Information Fig. S5A). Nonetheless, such observations are inconsistent with the declining or stable TOC concentrations we would expect if heterotrophic processes were dominating in these incubations. While contamination due to sample handling cannot be ruled out, we explore here the possibility of increased TOC between timepoints as a result of chemoautotrophic carbon fixation driven by nitrification. While these experiments were not designed to directly measure nitrification, there are several lines of evidence that lend support to this explanation. The most compelling evidence for nitrification is the DIN speciation in the lysate addition incubations after 1 month (Fig. 7A). A high proportion of accumulated DIN as NO_2^- + NO_3^- would

suggest a history of ammonia oxidation in a given incubation; we observed this pattern in the DCM Pro lysate incubations from the cyclone and neutral sea-state and in the DCM Ehux incubations from the cyclone and one anticyclone replicate. This is in contrast to the lysate incubations from 25 m, where the DIN was primarily NH_4^+. Not all incubations with this signature of past ammonia oxidation showed accumulated TOC, but all experiments that demonstrated a relative TOC accumulation had a high proportion of DIN as $NO_2^- + NO_3^-$. Additional support is provided by analyses of *amoA* gene abundances from the field samples collected across the eddy dipole (Fig. 6). In these samples, *amoA* gene abundances were minimal at 25 m but considerably higher in the DCM, particularly in the cyclonic eddy. While the process of nitrification cannot be directly inferred from *amoA* genes (reviewed in Tolar et al. 2016), the presence of the gene indicates the DCM incubation starting communities possessed the genetic potential to conduct the first step of the pathway, and that DCM incubations started with more abundant ammonia oxidizers. Finally, it is improbable that this increase is merely TOC contamination from airborne volatile organics, as all DCM incubations were stored in the same incubator yet the majority of them do not show such an increase in TOC, nor do the 25 m incubations that were stored in the neighboring incubator. In addition, duplicate TOC samples from the incubations were tightly replicated (Supporting Information Table S5).

This potential nitrification response has implications for both nitrogen and organic matter cycling. First, the observed DIN signature of past ammonia oxidation suggests a potential feedback between eddy-induced phytoplankton blooms and uplift of mesopelagic nitrifiers that could lead to a shortened nitrogen remineralization length scale within eddies. As a caveat, we conducted this experiment in the dark, which could facilitate a higher nitrification rate than would be expected in the field, as ammonia-oxidizing archaea appear light-sensitive (Merbt et al. 2012). On the three rosette casts conducted during daylight hours, the DCM was located between the 0.8% and 1.5% light level, suggesting in situ light conditions could have impacted the ammonia-oxidizing archaea. More importantly, by isolating the community in the dark for an extended period of time, we effectively removed competition from phytoplankton for ammonia and allowed the slow-growing nitrifiers to monopolize the DIN pool (Zakem et al. 2018).

The relative accumulation of TOC in these incubations suggests that organic matter was produced over the time course of the experiment, and that this newly created organic matter was not readily bioavailable, in contrast to the rapid remineralization of the added phytoplankton lysates. The apparent persistence of this TOC suggests that autotrophy by ammonia-oxidizing archaea and nitrite-oxidizing bacteria might produce organic matter that is not readily labile to catabolism by other bacterioplankton on short timescales, whether because it is contained in still-living biomass or because it is not metabolically accessible if released in dissolved form. The latter scenario is consistent with the findings of Bayer et al. (2019) that the exometabolomes of ammonia-oxidizing archaea contain a high proportion of presumably recalcitrant carboxyl-rich alicyclic molecules (i.e., CRAM). Conversely, the TOC accumulation could reflect catabolic byproducts of organic matter that had been produced by chemoautotrophy and subsequently subjected to heterotrophic processing by the 1-month sampling point. The bioavailability and composition of organic matter produced by nitrification-driven chemoautotrophy clearly deserve further study.

While the global importance of nitrification-based chemoautotrophy is well established on a broad scale for the euphotic and upper mesopelagic zones (Middelburg 2011; Santoro et al. 2019), little is known about the fate of this organic matter beyond the argument that it likely fuels heterotrophy to help satisfy mass-balance constraints below the photic zone (Reinthaler et al. 2010). Evidence supporting a pathway to heterotrophy is growing: cultured ammonia-oxidizing archaea have been shown to release DOM that can drive growth by heterotrophic bacterioplankton (Bayer et al. 2019), and, based on in situ associations, Reji et al. (2019) inferred a potential metabolic relationship between *Thaumarchaeota* and certain heterotrophic bacteria in a coastal upwelling system. Our results suggest that chemoautotrophy via nitrification could contribute semi-labile DOM in the upper mesopelagic that is indirectly derived from surface processes—consistent with, but mechanistically distinct from, the standard paradigm of increasingly reduced DOM bioavailability with depth due to heterotrophic processing (Hansell 2013). This would not constitute a net production of TOC (e.g., Supporting Information Fig. S5A), as the energy fueling nitrification originates from remineralized organic matter; rather, this process would represent internal cycling and transformation of organic matter, at a net loss of fixed C.

Finally, from a strictly methodological standpoint, these results suggest that bulk TOC remineralization measured in batch-culture bioassays, even those conducted in the dark, can be confounded by opposing biological processes to a measurable extent. We posit that tracking DIN speciation over multiple timepoints is the simplest way to distinguish potential nitrification-driven chemoautotrophy from contamination in long-term experiments from environments where this pathway is a possibility, though it does not provide a quantitative assessment of rates.

Long-term remineralization: Priming of ambient DOM

The low bioavailability of organic matter in the ambient controls is consistent with our expectations for the euphotic zone of an oligotrophic gyre under stratified conditions (Carlson et al. 2002; Carlson et al. 2004; Hansell 2013). However, our lysate addition incubations suggest that a portion of the ambient DOM can be utilized when conditions change. We saw evidence for priming (that is, the remineralization of presumably

semi-labile DOM facilitated by growth and enzymatic production upon a more labile substrate; Guenet et al. 2010) in at least one replicate from most 25 m incubations (Fig. 7C). While inorganic nutrients added with the lysate could likewise stimulate uptake of ambient DOM, the putative priming effect was observed in incubations of both lysate types, and the Pro lysate amendments did not add measurable inorganic nutrients. It would also be stoichiometrically improbable to stimulate the observed excess TOC remineralization (>3 μM in several incubations) based on concentrations of inorganic nitrogen and phosphate present below the method detection limits (< 0.1 or 0.2 μM). We note that priming could be occurring in incubations from the DCM as well; however, as priming and chemoautotrophy would have opposing effects on TOC concentrations, we might not be able to detect it consistently at this depth.

TOC priming (defined here as remineralization exceeding the sum of TOC added as lysate and remineralization measured in the corresponding ambient DOM incubations; Supporting Information Fig. S6) was detected in six (of 12) 25 m, lysate addition replicates (Fig. 7C), where TOC removal was between 2.0 and 5.5 μM greater than the amount of lysate TOC added. This is similar in magnitude to the 1 to 5 μM priming of upper water column TOC utilization observed over 1–2 months in bioassays from the Sargasso Sea, which in that case was triggered by model compounds (Carlson et al. 2002). As this approach to calculating priming considers only TOC that was remineralized and not ambient DOM that may have been incorporated into biomass, it represents a minimum estimate of a priming effect. We observed no clear relationship between TOC priming and eddy location, consistent with the lack of observed physicochemical eddy effects in the surface waters (Fig. 2). The poor replication between duplicate incubations suggests that priming involves a biological response in the community that requires specific physiological processes or phylogenetic changes to occur, rather than being a foregone conclusion of added energy or limiting nutrients such as nitrogen. The observed TOC priming suggests that phytoplankton blooms stimulated by eddy upwelling could impact heterotrophic carbon cycling in the gyres beyond simply the short-term input of labile energy sources; indirectly, they might provide an impetus for biological turnover of accumulated semi-labile DOM.

Conclusions

Bacterioplankton community metabolic potential across the eddy dipole did not show the hypothesized spatial specialization toward lysates generated from different phytoplankton types. Rather, communities across the eddy dipole maintained the metabolic potential to respond similarly to each respective lysate type. However, we cannot eliminate the possibility that such an effect exists in an eddy dipole with a more extreme biogeochemical gradient. We further observed evidence that eddies, and the associated transient increases in labile substrates they produce, could impact the production and consumption of semi-labile DOM in the stratified gyre. Lysate additions primed remineralization of semi-labile ambient DOM in the 25 m experiments, while chemoautotrophy fueled by nitrification appeared to underlie an accumulation of TOC in some DCM experiments. Together, such results suggest that mesoscale-linked physical dynamics can have complex direct and indirect impacts on bacterioplankton metabolism and ecology.

Data availability

Amplicon sequences are available through the National Center for Biotechnology Information Sequence Read Archive (https://www.ncbi.nlm.nih.gov/sra; accession number PRJNA528517). All biogeochemical field and experimental results unique to this study are included in Supporting Information Tables S4 and S5.

References

Amin, S. A., M. S. Parker, and E. V. Armbrust. 2012. Interactions between diatoms and bacteria. Microbiol. Molec. Biol. Rev. **76**: 667–684. doi:10.1128/MMBR.00007-12

Ascani, F., K. J. Richards, E. Firing, S. Grant, K. S. Johnson, Y. Jia, R. Lukas, and D. M. Karl. 2013. Physical and biological controls of nitrate concentrations in the upper subtropical North Pacific Ocean. Deep-Sea Res. II **93**: 119–134. doi:10.1016/j.dsr2.2013.01.034

Asplund, M. E., A.-S. Rehnstam-Holm, V. Atnur, P. Raghunath, V. Saravanan, K. Härnström, B. Collin, I. Karunasagar, and A. Godhe. 2011. Water column dynamics of *Vibrio* in relation to phytoplankton community composition and environmental conditions in a tropical coastal area. Environ. Microbiol. **13**: 2738–2751. doi:10.1111/j.1462-2920.2011.02545.x

Baltar, F., J. Arístegui, J. M. Gasol, I. Lekunberri, and G. J. Herndl. 2010. Mesoscale eddies: Hotspots of prokaryotic activity and differential community structure in the ocean. ISME J. **4**: 975–988. doi:10.1038/ismej.2010.33

Barone, B., A. R. Coenen, S. J. Beckett, D. J. McGillicuddy Jr., J. S. Weitz, and D. M. Karl. 2019. The ecological and biogeochemical state of the North Pacific subtropical gyre is linked to sea surface height. The Sea: The Current and Future Ocean. J. Mar. Res. **77**(S): 215-245.

Bayer, B., R. L. Hansman, M. J. Bittner, B. E. Noriega-Ortega, J. Niggemann, T. Dittmar, and G. J. Herndl. 2019. Ammonia-oxidizing archaea release a suite of organic compounds potentially fueling prokaryotic heterotrophy in the ocean. Environ. Microbiol. **21**: 4062–4075. doi:10.1111/1462-2920.14755

Becker, J. W., P. M. Berube, C. L. Follett, J. B. Waterbury, S. W. Chisholm, E. F. DeLong, and D. J. Repeta. 2014. Closely related phytoplankton species produce similar suites of dissolved organic matter. Front. Microbiol. **5**: 111. doi:10.3389/fmicb.2014.00111

Beman, J. M., B. N. Popp, and C. A. Francis. 2008. Molecular and biogeochemical evidence for ammonia oxidation by marine Crenarchaeota in the Gulf of California. ISME J. **2**: 429–441. doi:10.1038/ismej.2007.118

Benitez-Nelson, C. R., and others. 2007. Mesoscale eddies drive increased silica export in the subtropical Pacific Ocean. Science **316**: 1017–1021. doi:10.1126/science.1136221

Benitez-Nelson, C. R., and D. J. McGillicuddy Jr. 2008. Mesoscale physical-biological-biogeochemical linkages in the open ocean: An introduction to the results of the E-flux and EDDIES programs. Deep-Sea Res. II **55**: 1133–1138. doi:10.1016/j.dsr2.2008.03.001

Caporaso, J. G., and others. 2012. Ultra-high-throughput microbial community analysis on the Illumina HiSeq and MiSeq platforms. ISME J. **6**: 1621–1624. doi:10.1038/ismej.2012.8

Carlson, C. A., S. J. Giovannoni, D. A. Hansell, S. J. Goldberg, R. Parsons, M. P. Otero, K. Vergin, and B. R. Wheeler. 2002. Effect of nutrient amendments on bacterioplankton production, community structure, and DOC utilization in the Northwest Sargasso Sea. Aquat. Microb. Ecol. **30**: 19–36. doi:10.3354/ame030019

Carlson, C. A., S. J. Giovannoni, D. A. Hansell, S. J. Goldberg, R. Parsons, and K. Vergin. 2004. Interactions among dissolved organic carbon, microbial processes, and community structure in the mesopelagic zone of the northwestern Sargasso Sea. Limnol. Oceanogr. **49**: 1073–1083. doi:10.4319/lo.2004.49.4.1073

Carlson, C. A., and D. A. Hansell. 2015. DOM sources, sinks, reactivity, and budgets. *In* D. A. Hansell and C. A. Carlson [eds.], Biogeochemistry of marine dissolved organic matter, 2nd ed. Academic Press. doi:10.1002/2015JD023849

Chen, F., W.-J. Cai, Y. Wang, Y. M. Rii, R. R. Bidigare, and C. R. Benitez-Nelson. 2008. The carbon dioxide system and net community production within a cyclonic eddy in the lee of Hawaii. Deep-Sea Res. **II**: 1412–1425. doi:10.1016/j.dsr2.2008.01.011

Christian, J. R., and D. M. Karl. 1994. Microbial community structure at the U.S.-Joint Global Ocean Flux Study Station ALOHA: Inverse methods for estimating biochemical indicator ratios. J. Geophys. Res. **99**: 14269–14276. doi:10.1029/94JC00681

Church, M. J., C. Mahaffey, R. M. Letelier, R. Lukas, J. P. Zehr, and D. M. Karl. 2009. Physical forcing of nitrogen fixation and diazotroph community structure in the North Pacific subtropical gyre. Global Biogeochem. Cycles **23**: GB2020. doi:10.1029/2008GB003418

Clarke, K. R., and R. N. Gorley. 2006. PRIMER v6: user manual/tutorial. New Brunswick, Canada: PRIMER-E. doi:10.1109/IEMBS.2006.260840

Cortés, M. Y., J. Bollmann, and H. R. Thierstein. 2001. Coccolithophore ecology at the HOT station ALOHA, Hawaii. Deep-Sea Res. II **48**: 1957–1981. doi:10.1016/S0967-0645(00)00165-X

Cotti-Rausch, B. E., M. W. Lomas, E. M. Lachenmyer, E. A. Goldman, D. W. Bell, S. R. Goldberg, and T. L. Richardson. 2016. Mesoscale and sub-mesoscale variability in phytoplankton community composition in the Sargasso Sea. Deep-Sea Res. I **110**: 106–122. doi:10.1016/j.dsr.2015.11.008

Dittmar, T., B. Koch, N. Hertkorn, and G. Kattner. 2008. A simple and efficient method for the solid-phase extraction of dissolved organic matter (SPE-DOM) from seawater. Limnol. Oceanogr. Methods **6**: 230–235. doi:10.4319/lom.2008.6.230

Ewart, C. S., M. K. Meyers, E. R. Wallner, D. J. McGillicuddy Jr., and C. A. Carlson. 2008. Microbial dynamics in cyclonic and anti-cyclonic mode-water eddies in the northwestern Sargasso Sea. Deep-Sea Res. II **55**: 1334–1347. doi:10.1016/j.dsr2.2008.02.013

Fong, A. A., D. M. Karl, R. Lukas, R. M. Letelier, J. P. Zehr, and M. J. Church. 2008. Nitrogen fixation in an anticyclonic eddy in the oligotrophic North Pacific Ocean. The ISME J. **2**: 663–676. doi:10.1038/ismej.2008.22

Fukuda, R., H. Ogawa, T. Nagata, and I. Koike. 1998. Direct determination of carbon and nitrogen contents of natural bacterial assemblages in marine environments. Appl. Environ. Microbiol. **64**: 3352–3358. doi:10.1128/aem.64.9.3352-3358.1998

Gilbert, J. A., and others. 2012. Defining seasonal marine microbial community dynamics. ISME J. **6**: 298–308. doi:10.1038/ismej.2011.107

del Giorgio, P. A., and J. J. Cole. 1998. Bacterial growth efficiency in natural aquatic systems. Annu. Rev. Ecol. Syst. **29**: 503–541. doi:10.1146/annurev.ecolsys.29.1.503

Guenet, B., M. Danger, L. Abbadie, and G. Lacroix. 2010. Priming effect: Bridging the gap between terrestrial and aquatic ecology. Ecology **91**: 2850–2861. doi:10.1890/09-1968.1

Hansell, D. A. 2005. Dissolved organic carbon reference material program. Eos **86**: 318. doi:10.1029/2005EO350003

Hansell, D. A. 2013. Recalcitrant dissolved organic carbon fractions. Ann. Rev. Mar. Sci. **5**: 421–445. doi:10.1146/annurev-marine-120710-100757

James, A. K., U. Passow, M. A. Brzezinski, R. J. Parsons, J. N. Trapani, and C. A. Carlson. 2017. Elevated pCO_2 enhances bacterioplankton removal of organic carbon. PLoS ONE **12**: e0173145. doi:10.1371/journal.pone.0173145

Johnson, K. S., S. C. Riser, and D. M. Karl. 2010. Nitrate supply from deep to near-surface waters of the North Pacific subtropical gyre. Nature **465**: 1062–1065. doi:10.1038/nature09170

Karl, D. M., R. R. Bidigare, and R. M. Letelier. 2001. Long-term changes in plankton community structure and productivity in the North Pacific subtropical gyre: The domain shift

hypothesis. Deep-Sea Res. II **48**: 1449–1470. doi:10.1016/S0967-0645(00)00149-1

Kirchman, D. L. 1990. Limitation of bacterial growth by dissolved organic matter in the subarctic Pacific. Mar. Ecol. Prog. Ser. **62**: 47–54. doi:10.3354/meps062047

Ladd, T. M., J. A. Bullington, P. G. Matson, R. M. Kudela, and M. D. Iglesias-Rodríguez. 2018. Exposure to oil from the 2015 Refugio spill alters the physiology of a common harmful algal bloom species, *Pseudo-nitzschia australis*, and the ubiquitous coccolithophore, *Emiliana huxleyi*. Mar. Ecol. Prog. Ser. **603**: 61–78. doi:10.3354/meps12710

Letelier, R. M., D. M. Karl, M. R. Abbott, P. Flament, M. Freilich, R. Lukas, and T. Strub. 2000. Role of late winter mesoscale events in the biogeochemical variability of the upper water column of the North Pacific subtropical gyre. J. Geophys. Res. **105**: 28723–28739. doi:10.1029/1999JC000306

Lochte, K., and O. Pfannkuche. 1987. Cyclonic cold-core eddy in the eastern North Atlantic. II. Nutrients, phytoplankton, and bacterioplankton. Mar. Ecol. Prog. Ser. **39**: 153–164. doi:10.3354/meps039153

Lozupone, C., and R. Knight. 2005. UniFrac: A new phylogenetic method for comparing microbial communities. Appl. Environ. Microbiol. **71**: 8228–8235. doi:10.1128/AEM.71.12.8228-8235.2005

Main, C. R., L. R. Salvitti, E. B. Whereat, and K. J. Coyne. 2015. Community-level and species-specific associations between phytoplankton and particle-associated *Vibrio* species in Delaware's inland bays. Appl. Environ. Microbiol. **81**: 5703–5713. doi:10.1128/AEM.00580-15

McCarren, J., J. W. Becker, D. J. Repeta, Y. Shi, C. R. Young, R. R. Malmstrom, S. W. Chisholm, and E. F. DeLong. 2010. Microbial community transcriptomes reveal microbes and metabolic pathways associated with dissolved organic matter turnover in the sea. PNAS **107**: 16420–16427. doi:10.1073/pnas.1010732107

McGillicuddy, D. J., Jr. 2016. Mechanisms of physical-biological-biogeochemical interaction at the oceanic mesoscale. Ann. Rev. Mar. Sci. **8**: 125–159. doi:10.1146/annurev-marine-010814-015606

McGillicuddy, D. J., Jr., A. R. Robinson, D. A. Siegel, H. W. Jannasch, R. Johnson, T. D. Dickey, J. McNiel, A. F. Michaels, and A. H. Knap. 1998. Influence of mesoscale eddies on new production in the Sargasso Sea. Nature **394**: 263–266. doi:10.1038/28367

Merbt, S. N., D. A. Stahl, E. O. Casamayor, E. Martí, G. W. Nicol, and J. I. Prosser. 2012. Differential photoinhibition of bacterial and archaeal ammonia oxidation. FEMS Microbiol. Lett. **327**: 41–46. doi:10.1111/j.1574-6968.2011.02457.x

Middelburg, J. J. 2011. Chemoautotrophy in the ocean. Geophys. Res. Lett. **38**: L24604. doi:10.1029/2011GL049725

Moore, L. R., A. Coe, E. R. Zinser, M. A. Saito, M. B. Sullivan, D. Lindell, K. Frois-Moniz, J. Waterbury, and S. W. Chisholm. 2007. Culturing the marine cyanobacterium *Prochlorococcus*. Limnol. Oceanogr. Methods **5**: 353–362. doi:10.4319/lom.2007.5.353

Nelson, C. E., and C. A. Carlson. 2012. Tracking differential incorporation of dissolved organic carbon types among diverse lineages of Sargasso Sea bacterioplankton. Environ. Microbiol. **14**: 1500–1516. doi:10.1111/j.1462-2920.2012.02738.x

Nelson, C. E., C. A. Carlson, C. S. Ewart, and E. R. Halewood. 2014. Community differentiation and population enrichment of Sargasso Sea bacterioplankton in the euphotic zone of a mesoscale mode-water eddy. Environ. Microbiol. **16**: 871–887. doi:10.1111/1462-2920.12241

Nelson, C. E., and E. K. Wear. 2014. Microbial diversity and the lability of dissolved organic carbon. PNAS **111**: 7166–7167. doi:10.1073/pnas.1405751111

Parada, A. E., D. M. Needham, and J. A. Fuhrman. 2016. Every base matters: Assessing small subunit rRNA primers for marine microbiomes with mock communities, time series and global field samples. Environ. Microbiol. **18**: 1403–1414. doi:10.1111/1462-2920.13023

Pedler, B. E., L. I. Aluwihare, and F. Azam. 2014. Single bacterial strain capable of significant contribution to carbon cycling in the surface ocean. PNAS **111**: 7202–7207. doi:10.1073/pnas.1401887111

Quast, C., E. Pruesse, P. Yilmaz, J. Gerken, T. Schweer, P. Yarza, J. Peplies, and F. O. Glöckner. 2013. The SILVA ribosomal RNA gene database project: Improved data processing and web-based tools. Nucleic Acids Res. **41**: D590–D596. doi:10.1093/nar/gks1219

Reinthaler, T., H. M. van Aken, and G. J. Herndl. 2010. Major contribution of autotrophy to microbial carbon cycling in the deep North Atlantic interior. Deep-Sea Res. II **57**: 1572–1580. doi:10.1016/j.dsr2.2010.02.023

Reji, L., B. B. Tolar, J. M. Smith, F. P. Chavez, and C. A. Francis. 2019. Differential co-occurrence relationships shaping ecotype diversification within *Thaumarchaeota* populations in the coastal ocean water column. ISME J. **13**: 1144–1158. doi:10.1038/s41396-018-0311-x

Rii, Y. M., S. L. Borwn, F. Nencioli, V. Kuwahara, T. Dickey, D. M. Karl, and R. R. Bidigare. 2008. The transient oasis: Nutrient-phytoplankton dynamics and particle export in Hawaiian lee cyclones. Deep-Sea Res. II **55**: 1275–1290. doi:10.1016/j.dsr2.2008.01.013

Santoro, A. E., R. A. Richter, and C. L. Dupont. 2019. Planktonic marine archaea. Ann. Rev. Mar. Sci. **11**: 131–158. doi:10.1146/annurev-marine-121916-063141

Sarmento, H. S., and J. M. Gasol. 2012. Use of phytoplankton-derived dissolved organic carbon by different types of bacterioplankton. Environ. Microbiol. **14**: 2348–2360. doi:10.1111/j.1462-2920.2012.02787.x

Schlitzer, R. 2018. Ocean Data View. https://odv.awi.de, DOI:10.12688/f1000research.14793.1

Schloss, P. D., and others. 2009. Introducing mothur: Open-source, platform-independent, community-supported software

for describing and comparing microbial communities. Appl. Environ. Microbiol. **75**: 7537–7541. doi:10.1128/AEM.01541-09

Sweeney, E. N., D. J. McGillicuddy Jr., and K. O. Buesseler. 2003. Biogeochemical impacts due to mesoscale eddy activity in the Sargasso Sea as measured at the Bermuda Atlantic time-series study (BATS). Deep Sea Res. II **50**: 3017–3039. doi:10.1016/j.dsr2.2003.07.008

Thompson, J. R., and M. F. Polz. 2006. Dynamics of *Vibrio* populations and their role in environmental nutrient cycling. *In* F. L. Thompson, B. Austin, and J. Swings [eds.], Biology of Vibrios. ASM Press. doi:10.1128/9781555815714

Tolar, B. B., M. J. Ross, N. J. Wallsgrove, Q. Liu, L. I. Aluwihare, B. N. Popp, and J. T. Hollibaugh. 2016. Contribution of ammonia oxidation to chemoautotrophy in Antarctic coastal waters. ISME J. **10**: 2605–2619. doi:10.1038/ismej.2016.61

Vaillancourt, R. D., J. Marra, M. P. Seki, M. L. Parsons, and R. R. Bidigare. 2003. Impact of a cyclonic eddy on phytoplankton community structure and photosynthetic competency in the subtropical North Pacific Ocean. Deep-Sea Res. I **50**: 829–847. doi:10.1016/S0967-0637(03)00059-1

Wear, E. K., C. A. Carlson, L. A. Windecker, and M. A. Brzezinski. 2015. Roles of diatom nutrient stress and species identity in determining the short- and long-term bioavailability of diatom exudates to bacterioplankton. Mar. Chem. **177**: 335–348. doi:10.1016/j.marchem.2015.09.001

Yan, W., R. Zhang, and N. Jiao. 2018. A long-standing complex tropical dipole shapes marine microbial biogeography. Appl. Environ. Microbiol. **84**: e00614–e00618. doi:10.1128/AEM.00614-18

Zakem, E. J., A. Al-Haj, M. J. Church, G. L. van Dijken, S. Dutkiewicz, S. Q. Foster, R. W. Fulweiler, M. M. Mills, and M. J. Follows. 2018. Ecological control of nitrite in the upper ocean. Nat. Comms. **9**: 1206. doi:10.1038/s41467-018-03553-w

Zhang, R., R. L. Kelly, K. M. Kauffman, A. K. Reid, J. M. Lauderdale, M. J. Follows, and S. G. John. 2019. Growth of marine *Vibrio* in oligotrophic environments is not stimulated by the addition of inorganic iron. Earth Planet. Sci. Lett. **516**: 148–155. doi:10.1016/j.epsl.2019.04.002

Acknowledgments

This work was funded by the Simons Foundation through the Simons Collaboration on Ocean Processes and Ecology (SCOPE award #329108 to MJC), with additional support from Simons Foundation International's BIOS-SCOPE program to CAC. Ship time was funded by the Schmidt Ocean Institute. We thank Trista Vick-Majors, the SCOPE staff, Craig Nelson, and Wesley Sparagon for logistical and sampling assistance. *Prochlorococcus* cells were provided by Allison Coe and Penny Chisholm; *E. huxleyi* lysate was provided by Nicholas Baetge and Kara Newman. Shuting Liu generously quantified amino acids. Brandon Stephens provided advice on biovolume measurements. We thank Sam Wilson and the officers and crew of the R/V *Falkor* for assistance at sea. John Ranieri conducted ddPCR and Keri Opalk measured TOC and TN. Two anonymous reviewers and members of the SCOPE and BIOS-SCOPE projects provided valuable feedback on this work.

Conflict of Interest

None declared.

Submitted 31 May 2019
Revised 15 November 2019
Accepted 02 January 2020

Associate editor: Thomas Anderson